Towards accurate cosmological predictions for rapidly oscillating scalar fields as dark matter

L. Arturo Ureña-López[1,*] and Alma X. Gonzalez-Morales[1,2,†]

[1] *Departamento de Física, DCI, Campus León, Universidad de Guanajuato, 37150, León, Guanajuato, México.*
[2] *Consejo Nacional de Ciencia y Tecnología, Av. Insurgentes Sur 1582. Colonia Crédito Constructor, Del. Benito Jurez C.P. 03940, México D.F. México*

(Dated: November 26, 2015)

As we are entering the era of precision cosmology, it is necessary to count on accurate cosmological predictions from any proposed model of dark matter. In this paper we present a novel approach to the cosmological evolution of scalar fields that eases their analytic and numerical analysis at the background and at the linear order of perturbations. We apply the method to a scalar field endowed with a quadratic potential and revisit its properties as dark matter. Some of the results known in the literature are recovered, and a better understanding of the physical properties of the model is provided. It is shown that the Jeans wavenumber defined as $k_J = a\sqrt{mH}$ is directly related to the suppression of linear perturbations at wavenumbers $k > k_J$. We also discuss some semi-analytical results that are well satisfied by the full numerical solutions obtained from an amended version of the CMB code CLASS. Finally we draw some of the implications that this new treatment of the equations of motion may have in the prediction for cosmological observables.

PACS numbers: 98.80.-k,95.35.+d,98.80.Jk

arXiv:1511.08195v1 [astro-ph.CO] 25 Nov 2015

I. INTRODUCTION

The most recent observational results from the Cosmic Microwave Background (CMB) give strong support to the idea of a benchmark model of the Universe that is consistent with a variety of observational data[1]. It is remarkable that this standard model, well known as the ΛCDM model, is at its core just described by nine numbers with a true cosmological context; the rest of the physical quantities and constants can be fixed and measured by other methods at terrestrial laboratories.

One of the cosmological numbers is particularly important to understand the formation of cosmological structure: the actual amount of cold dark matter (CDM), $\Omega_c h^2 \simeq 0.119$. Dark matter represents about 27% of the total matter budget. The base model for CDM is as simple as it gets: a pressureless fluid of particles that have no direct, weak at most, interaction with other matter fluids apart from the gravitational one. These two basic properties are enough to provide a complex picture of structure formation through hierarchical assembling that fits data at different scales[2]. A detailed model of CDM is necessary, but so far observations seem not to be very demanding in that regard[3], and a direct detection of the dark matter particle in terrestrial laboratories does not yet seem feasible[4].

A satisfactory answer to the CDM riddle have to be complemented with a convincing theoretical model that give us a comprehensive understanding of its properties. Although there is quite a large number of proposals, here we will focus in a type of model that has been studied for more than two decades: scalar field dark matter (SFDM)[5–12]. The key concept in this model is that the dark matter properties can be described by the dynamics of a self-interacting real scalar field with a probably fundamental origin, and a very tiny mass of around 10^{-22} eV[13]. Cosmological scalar fields are better known in the context of dark energy models because many proposals are able to provide an accelerating expansion of the Universe at late times[14]; however, for dark matter models it has been widely shown that any successful model must be at the end related, somehow, to the simplest possible case: a scalar field potential with a parabolic shape around a minimum (see [15] for comprehensive reviews).

The typical form of the scalar field potential in SFDM models is:

$$V(\phi) = (1/2)m^2\phi^2\,, \tag{1}$$

where ϕ is a real scalar field, and m is its mass scale. As we said before, other potentials exist for SFDM models, but their common feature is that they all can be approximated by the functional form (1) once they enter the dark matter phase, see for instance[6–8, 12, 16]. The resultant behavior of scalar fields as a pressureless fluid appears from their rapid oscillations around the minimum of the potential (1), which is a well-known fact[17–19]. For rapid oscillations we mean that the period of the field oscillations, represented by the time scale m^{-1}, is much shorter than the typical Hubble time H^{-1} for the expansion of the Universe, where H is the Hubble parameter. Because the Hubble parameter is a decreasing function of time, the ratio m^{-1}/H^{-1} quickly becomes very small for realistic models, and then accurate numerical methods are required for a precise evolution of the equations of motion[15]. This difficulty has been overcome somehow by the use of approximate formulas, see for instance[7, 8, 12, 18, 20], that are intended to match

* lurena@fisica.ugto.mx
† alma.gonzalez@fisica.ugto.mx

as smoothly as possible the transition towards the pressureless phase of the scalar field dynamics (see also[21]).

As for any dark matter model, the properties of SFDM models must also be connected to the formation of structure in the Universe, and then the same physical properties that allow a consistent evolution at cosmological scales must also be appropriate for the development of realistic galaxy halos. The latter have been also extensively studied in the literature for SFDM models, see for instance[22–25] and references therein. More recently, complete N-body simulations have shown the similarities of SFDM with CDM[7, 26] at large scales, although most of these studies have been done under the non-relativistic approximation. One another quantity that plays an important role here is the mass power spectrum, which represents the aggregation properties of matter at different scales, whose measurement are for now in good agreement with the theoretical expectations of the ΛCDM model. Nonetheless, the mass power spectrum is sensitive to the physical properties of the dark matter particles, and there may be noticeable consequences in the history of galaxy formation if the dark matter component is not strictly cold, as has been shown in[7, 27, 28].

Given the interest in SFDM models in the recent literature, it is desirable to have an improved handling of their cosmological dynamics, for variables in the background and in linear perturbations, even if eventually one has to use numerical methods to resolve them completely. Along these lines, the aim in this paper is two fold. First, we would like to present a new approach for the solution of the cosmological equations of SFDM, so that we can have a proper understanding of the subtleties in their evolution. This will be achieved through the use of the tools of dynamical systems (for some pedagogical presentations see[29]), together with appropriate changes of variables that are more than suitable to exploit the intrinsic symmetries of the equations of motion. The techniques developed here can be easily extended to different cosmological settings in which scalar fields may be involved. Second, we will analyze the mass PS of SFDM models for different masses of the SFDM particle draw some implications on other observables such as the mass function, in a approximate way since the scales of interst are beyond the realm of linear perturbations.

A brief summary of the paper is as follows. In Sec. II we explain the conversion of the equations of motion for a scalar field dominated Universe into an autonomous dynamical system, where the latter is written in terms of a kinetic variable and two potential variables. Taking into account the symmetries of the system of equations, we propose a change to polar coordinates that helps to convert them into a more manageable 2-dimensional dynamical system that can be solved numerically without any by-hand manipulations. As we shall show, the new method is able to follow the evolution of the system from the early slow-roll regime to that of rapid oscillations with high precision and minimal numerical effort.

In Sec. III, we apply similar mathematical manipulations to the equations of motion of linear perturbations, so that their evolution is also given in terms of a 2-dimensional dynamical system. All the new equations, for the background and for linear perturbations, will be put into an amended version of CLASS[30], which will be used to calculate all relevant cosmological quantities. We will clearly identify, within the new system of equations, the so-called Jeans scale of SFDM. As a side result, the velocity gradient is also calculated to verify the appropriateness of the synchronous gauge for the calculation of linear perturbations of SFDM models.

In Sec. V, we will analyze the suppression of power in the mass power spectrum and discuss the possibilities to constrain the model with current and future galaxy surveys. We will also discuss, from a qualitatively point of view, the effect of the aforementioned suppression in the nowadays mass function of halos. Finally, Sec. VI will be devoted to a general discussion of the main results and conclusions.

II. SFDM BACKGROUND DYNAMICS

For the background dynamics, we shall consider a spatially-flat Universe populated with standard matter fluids such as: radiation, neutrinos, baryons, a cosmological constant, together with dark matter described by a scalar field ϕ endowed with the quadratic potential (1). We will refer to the model as ΛSFDM, to emphasize the role of the scalar field as dark matter, with Λ still playing the role of dark energy.

A. Mathematical background

The energy density ρ_j and pressure p_j for each matter fluid, represented here by the label i, are related through the barotropic relation $p_j = w_j \rho_j$, where w_j is their corresponding equation of state (EoS). Hence, the full equations of motion of the ΛSFDM model are:

$$H^2 = \frac{\kappa^2}{3}\left(\sum_j \rho_j + \rho_\phi\right) , \tag{2a}$$

$$\dot{H} = -\frac{\kappa^2}{2}\left[\sum_j (\rho_j + p_j) + (\rho_\phi + p_\phi)\right] , \tag{2b}$$

$$\dot{\rho}_j = -3H(\rho_j + p_j) , \tag{2c}$$

$$\ddot{\phi} = -3H\dot{\phi} - m^2\phi , \tag{2d}$$

where $\kappa^2 = 8\pi G$, a dot denotes derivative with respect to cosmic time t, and H is the Hubble parameter. The scalar field energy density ρ_ϕ and pressure p_ϕ are given by the known expressions:

$$\rho_\phi = \frac{1}{2}\dot{\phi}^2 + \frac{1}{2}m^2\phi^2 , \quad p_\phi = \frac{1}{2}\dot{\phi}^2 - \frac{1}{2}m^2\phi^2 . \tag{3}$$

In order to transform the Klein-Gordon (KG) equation (2d), we define a new set of variables[31]:

$$x \equiv \frac{\kappa\dot{\phi}}{\sqrt{6}H}\,, \quad y \equiv -\frac{\kappa m\phi}{\sqrt{6}H}\,, \quad y_1 \equiv 2\frac{m}{H}\,, \tag{4}$$

In writing the definition of the new variable y_1, we are assuming that initially $\phi < 0$. As a result, the KG equation can be written as a system of first order differential equations in the form:

$$x' = -\left(3 + \frac{\dot{H}}{H^2}\right)x + \frac{1}{2}yy_1\,, \tag{5a}$$

$$y' = -\frac{\dot{H}}{H^2}y - \frac{1}{2}xy_1\,, \tag{5b}$$

$$y_1' = -\frac{\dot{H}}{H^2}y_1\,, \tag{5c}$$

where a prime denotes derivative with respect to the number of e-foldings $N \equiv \ln(a/a_i)$, with (a_i) a the (initial) scale factor of the Universe. (Hereafter, we label initial conditions with a sub-index i.)

We now apply a *polar* change of variables to the kinetic and potential variables in the form: $x = \Omega_\phi^{1/2}\sin(\theta/2)$ and $y = \Omega_\phi^{1/2}\cos(\theta/2)$, where $\Omega_\phi \equiv \kappa^2\rho_\phi/3H^2$ is the density parameter of the scalar field. This type of transformations was first proposed in[32], but see also[33] for other similar definitions. Firstly, we rewrite the Friedman constraint (2a) and the acceleration equation (2b), respectively, as

$$1 = \sum_j \Omega_j + \Omega_\phi\,, \quad \frac{\dot{H}}{H^2} = -\frac{3}{2}\left(1 + w_{tot}\right)\,, \tag{6a}$$

where

$$\Omega_j \equiv \frac{\kappa^2\rho_j}{3H^2}\,, \quad w_{tot} \equiv \frac{p_{tot}}{\rho_{tot}} = \sum_j \Omega_j w_j + \Omega_\phi w_\phi\,. \tag{6b}$$

Notice that we have defined the total EoS w_{tot} for the background dynamics in terms of the ratio of the total pressure p_{tot} to the total energy density ρ_{tot}, whereas that of the scalar field is simply given by

$$w_\phi \equiv \frac{p_\phi}{\rho_\phi} = \frac{x^2 - y^2}{x^2 + y^2} = -\cos\theta\,. \tag{7}$$

That is, the new angular variable θ is directly related to the scalar field EoS.

After some straightforward algebra, the KG equation (2d) becomes:

$$\theta' = -3\sin\theta + y_1\,, \tag{8a}$$

$$y_1' = \frac{3}{2}\left(1 + w_{tot}\right)y_1\,, \tag{8b}$$

$$\Omega_\phi' = 3(w_{tot} - w_\phi)\Omega_\phi\,. \tag{8c}$$

Eqs. (8) are a compact and neat representation of the KG equation, and they reveal that the true variables driving the scalar field dynamics are $(\theta, y_1, \Omega_\phi)$, with the field values ϕ and $\dot{\phi}$ now playing a secondary role. Eqs. (8) also show that the dynamics of the quadratic potential does not have any free physical parameters, as the successive transformations applied to the KG equation made the field mass m become an implicit parameter in the final equations of motion.

B. Early, intermediate, and late time behaviors

It is convenient to study the behavior of the scalar field under the new equations of motion. (8). For that we consider that there is a special time for the beginning of the scalar field oscillations around the minimum of the potential (1), that we will denote by its corresponding scale factor a_{osc}. Equivalently, a_{osc} also corresponds to $\theta_{osc} = \pi/2$, which is the point at which the SFDM EoS first passes through zero, $w_\phi(\theta_{osc}) = 0$.

As the field in our study will be part of the matter budget, we will also consider that the oscillations start before the time of radiation-matter equality, and then we put the constraint $a_{osc} < a_{eq}$. Thus, for early times we will refer to the epoch of radiation domination (RD) before the onset of the scalar field oscillations, so that $a \ll a_{osc}$. Intermediate times will refer to $a < a_{osc}$, still within the RD, whereas late times will strictly refer to $a > a_{osc}$. In terms of the angular variable θ, the above times can be rephrased as: $\theta \ll \pi/2$ for early times, $\theta < \pi/2$ for intermediate times, and $\theta > \pi/2$ for late times.

Before proceeding further, we note that in our scheme the SFDM mass can be determined from the initial condition of the second potential variable as: $m = y_{1i}H_i/2$, see also Eqs. (4). In general terms, we can expect that at early enough times $m/H_i \ll 1$, which directly indicates also that $y_{1i} \ll 1$. In terms of the original KG equation (2d), this implies that the scalar field dynamics is dominated by the friction term containing the Hubble parameter H, which then puts the field into a slow-roll phase with its energy density dominated by the potential term; this in turn translates into $x \ll y$, and then for the angular variable: $\theta_i \ll 1$. A similar result is expected for $\Omega_{\phi i} \ll 1$ if SFDM is to be subdominant during RD.

The above simple estimations indicate that the scalar field variables must have initial values very close to the following critical point of the dynamical system (8): $(\theta = 0, y_1 = 0, \Omega_\phi = 0)$. Under this assumption, Eqs. (8) can be linearised around this critical point as:

$$\theta' \simeq -3\theta + y_1\,, \quad y_1' \simeq 2y_1\,, \quad \Omega_\phi' \simeq 4\Omega_\phi\,, \tag{9}$$

where we have considered that $w_{tot} = 1/3$, as expected in RD, and also that $w_\phi \simeq -1$ and $\sin\theta \simeq \theta$ for $\theta \ll 1$. The linear system (9) has the following solutions in terms of

the scale factor a:

$$\theta = (1/5)y_1 + C(a/a_i)^{-3}\,, \tag{10a}$$
$$y_1 = y_{1i}(a/a_i)^2\,, \tag{10b}$$
$$\Omega_\phi = \Omega_{\phi i}(a/a_i)^4\,, \tag{10c}$$

with C an integration constant. The angular variable θ has growing and decaying modes, and when the latter disappears we find that $5\theta \simeq y_1$. We shall call this relation the *attractor solution* at early times between variables θ and y_1. As for the scalar field density parameter, its solution (10c) indicates that the SFDM energy density is constant during RD: $\rho_\phi \simeq \Omega_\phi \rho_r = \text{const}$.

For intermediate times, a more general solution of Eqs. (8a) and (8b) can be found perturbatively, as θ and y_1 remains reasonably small up to the time before the onset of oscillations at $\theta = \pi/2$. Moreover, θ has a monotonic behavior, and then we can propose the ansatz:

$$y_1(\theta) = \sum_{j=1} k_j \theta^j\,, \quad k_j = \text{const.} \tag{11}$$

We would like to emphasize that $y_1(\theta)$ is all that is needed to find a full solution of the scalar field equations (2). Indeed, once with the values of k_j at hand we can write Eq. (8a) as:

$$\theta' = (k_1 - 3)\theta + k_2\theta^2 + (k_3 + 1/2)\theta^3 + \dots\,. \tag{12}$$

Eq. (12) can in principle be integrated at any desired order in θ. For our purposes, it is enough to consider in Eq. (7) an expansion up to the third order, and then $y_1(\theta) = k_1\theta + k_2\theta^2 + k_3\theta^3$. The key step to find the coefficients k_{1j} is to write Eq. (8b) in the form

$$y_1' = \frac{dy_1}{d\theta}\theta' = \frac{dy_1}{d\theta}(-3\sin\theta + y_1) = 2y_1\,, \tag{13}$$

where we again assummed RD with $w_{tot} = 1/3$ for the last term on the rhs. After expanding both sides of Eq. (13) in powers of θ, the resultant polynomials must have the same coefficients, and from this condition we obtain $k_1 = 5$, $k_2 = 0$, and $k_3 = -5/18$. Finally, Eq. (12) can be integrated to find:

$$\frac{\theta^2}{\theta_i^2}\left(\frac{9+\theta_i^2}{9+\theta^2}\right) = (a/a_i)^4\,, \tag{14}$$

which could be easily inverted to find $\theta = \theta(a)$ for $a < a_{osc}$. If necessary, we can also calculate $y_1(a) = 5\theta(a) - 5\theta^3(a)/18$, whereas Ω_ϕ would still be given by Eq. (10c).

At late times $a > a_{osc}$, the scalar field field starts to oscillate rapidly around the minimum of the potential with a decreasing amplitude, and then we expect y_1 to grow very quickly and to become the dominant term in Eq. (8a): $\theta' \simeq y_1$. Changing back the derivative in the latter equation to the cosmic time t, we find that:

$$\dot\theta \simeq 2m \to \theta \simeq 2mt\,, \quad \text{and} \quad w_\phi \simeq -\cos(2mt)\,. \tag{15}$$

Irrespective of the domination era after the onset of oscillations, we can see that the SFDM EoS will oscillate around zero with a fixed frequency, in terms of the cosmic time, given by the field mass m. The oscillations happen in a time scale much smaller than that of the expansion rate of the Universe, which means that $H^{-1} > m^{-1}$. The Hubble parameter is a decreasing function of time, and we can only expect that $y_1 = 2m/H \gg 1$ as the Universe continues its expansion for $a > a_{osc}$.

For this reason, it is generically considered that the SFDM energy density evolves, on average, with a matter-like EoS: $\langle w_\phi \rangle \simeq 0$[17, 18]. This expectation has also been confirmed by accurate numerical simulations[6, 7, 15] (see also Fig. 7 in the Appendix A), and then we can safely take for granted that the SFDM background density will evolve as a matter component, $\rho_\phi \propto a^{-3}$, irrespectively of the presence of other fluid components.

C. Initial conditions

In order to find numerical solutions of the dynamical system (8), all that remains is to find appropriate initial conditions $(\theta_i, y_{1i}, \Omega_{\phi i})$, so that we can get the desired SFDM contribution $\Omega_{\phi 0}$ at the present time. This is done in most CMB codes, in terms of the standard field scheme, by the implementation of a shooting procedure to determine the correct initial values ϕ_i and $\dot\phi_i$[30]. However, it is still necessary to find a guess value, commonly obtained trough a cumbersome calculation[7, 20], to initiate the shooting method. As we shall show below, there is a more direct path to find the correct initial conditions in terms of our new dynamical variables.

We start by writing down an equation for the initial value of the SFDM density parameter $\Omega_{\phi i}$. For that, we first recall that once the scalar field starts to oscillate rapidly, its energy density redshifts as a^{-3}, so that its ratio with respect to the radiation component is: $\Omega_\phi/\Omega_r = (\Omega_{\phi 0}/\Omega_{r0})a$ for $a > a_{osc}$. In particular, we can write $\Omega_{\phi\, osc} \simeq a_{osc}\Omega_{rosc}(\Omega_{\phi 0}/\Omega_{r0}) \simeq a_{osc}(\Omega_{\phi 0}/\Omega_{r0})$, where the last expression takes into account that $\Omega_{rosc} = 1$ if the Universe is still dominated by radiation at $a = a_{osc}$. From Eq. (10c), we also know that $\Omega_{\phi\, osc} \simeq (a_{osc}/a_i)^4\Omega_{\phi i}$, and all together with Eq. (14) we finally find that:

$$\Omega_{\phi i} \simeq a_i\frac{\Omega_{\phi 0}}{\Omega_{r0}}\left(\frac{a_i}{a_{osc}}\right)^3 = a_i\frac{\Omega_{\phi 0}}{\Omega_{r0}}\left[\frac{4\theta_i^2}{\pi^2}\left(\frac{9+\pi^2/4}{9+\theta_i^2}\right)\right]^{3/4}. \tag{16}$$

The search for good initial conditions is now quite simple. We first need to set up by hand the desired contributions of the radiation and the SFDM components at the present time: Ω_{r0}, $\Omega_{\phi 0}$, together with the initial value of the scale factor a_i. Then, we choose an initial value θ_i, use the attractor solution of Eq. (10a) at early times to find: $y_{1i} = 5\theta_i$, and finally take Eq. (16) to find the corresponding initial value $\Omega_{\phi i}$.

To conclude this section, it must be said that the ratio

of the SFDM mass to the initial Hubble parameter is a *derived* value calculated from the initial conditions: in terms of the attractor relation for the potential variable y_1, we find that $m/H_i = y_{1i}/2 = (5/2)\theta_i$. A more useful formula can be written in terms of the present Hubble parameter H_0 as:

$$\frac{m}{H_0} = \frac{H_i}{H_0}\frac{y_{1i}}{2} = \frac{5}{2}\Omega_{r0}^{1/2} a_i^{-2}\theta_i \,, \tag{17}$$

where we have again assumed RD in the form $H_i^2 = (\kappa^2/3)\rho_{r0}a_i^{-4}$ to write the last expression on the rhs. Eq. (17) shows again the interplay of the initial conditions to set the value of the scalar field mass: everything else the same, different masses m are just obtained by taking different values of the initial condition θ_i.

D. Modifications in CLASS

The scheme described above to evolve the scalar field equations of motion was incorporated in an amended version of the freely-available code CLASS[30, 33][1]. In order to be consisten with the background evolution of other matter components within CLASS, the scalar field energy density and pressure were calculated, respectively, from the expressions:

$$\rho_\phi = \frac{\Omega_\phi}{1-\Omega_\phi}(\rho_r + \rho_m + \rho_\Lambda)\,, \quad p_\phi = -\cos\theta\cdot\rho_\phi\,. \tag{18}$$

The above formulae are found under the assumption that $\Omega_\phi = \rho_\phi/\rho_{tot}$, where ρ_{tot} is the total energy density at any given time. This assumption is in agreement with a spatially flat Universe, for which the total energy density coincides with the critical one $\rho_{tot} = \rho_{crit} = 3H^2/8\pi G$.

Even though Eqs. (8) are more convenient for accurate numerical solutions than the traditional field approach, they still require a highly efficient solver of differential equations to deal properly with the numerical stiffness of the scalar field oscillations. In order to circumvent this difficulty, we implemented a cut-off procedure on the trigonometric functions in the form:

$$\{\cos_\star\alpha, \sin_\star\alpha\} \equiv (1/2)\left[1-\tanh(\alpha^2-\alpha_\star^2)\right]\{\cos\alpha, \sin\alpha\}\,, \tag{19}$$

and then $\{\cos_\star\alpha, \sin_\star\alpha\} \to 0$ for $\alpha > \alpha_\star$. The threshold value $\alpha_\star$ was chosen empirically to neglect the trigonometric functions everywhere once the equation solver in CLASS was no longer able to keep an accurate track of the rapid oscillations of the scalar field. After some experimentation, we found that a convenient value is $\alpha_\star = 10^2$.

An illustrative physical example is the scalar field EoS, which was written inside CLASS as: $w_\phi = -\cos_\star\theta$. As we saw in Sec. II B, during the phase of rapid oscillations $\theta \simeq y_1 \simeq m/H$, and then in this case the threshold value $\alpha_\star$ means $\theta_\star \simeq m/H_\star \simeq 10^2$. In other words, w_ϕ is set to zero once the time scale for the expansion of the Universe is two orders of magnitude larger than the period of one oscillation in the EoS. As explained in more detail in the Appendix A, the implemented numerical cut-off (19) worked well, and did not introduce spurious effects into the numerical solutions.

As for the initial conditions, it must be said that Eq. (16) is not quite the correct initial condition for the SFDM density parameter, and we still needed to finely tune $\Omega_{\phi i}$ at the beginning of every numerical run. For that, we wrote $\Omega_{\phi i} = A\times$Eq. (16), where the value of A was adjusted with the shooting method already implemented within CLASS for scalar field models. A few iterations of the shooting routine were always enough to find the correct $\Omega_{\phi i}$ that leads to the desired $\Omega_{\phi 0}$ with a very high precision; in all instances it was found that $A = \mathcal{O}(1)$.

E. Numerical results for the background

Some numerical results from CLASS of background quantities are shown in Figs. 1, for a Universe in which the scalar field is the only dark matter component, that is, $\Omega_{\phi 0} = \Omega_{CDM0}$, whereas all other matter components (radiation, baryons, and Λ) are the same as reported by the Planck collaboration for the concordance model ΛCDM[34]. The mass of the SFDM particle in the given examples is indicated in the plots, and in each case was calculated from the initial condition θ_i through Eq. (17).

A general feature in all the numerical examples is that the SFDM energy density ρ_ϕ is constant at very early times, when its dynamics is dominated by its potential energy. Once the oscillations start, the energy density scales as a matter component, and the evolution of the density parameters clearly show that the subsequent epochs of matter and Λ domination are indistinguishable from those of ΛCDM. The onset of oscillations can be clearly seen in the evolution of the density parameters Ω, specially in the cases with the lightest masses. Actually, the oscillations start well before the time of radiation-matter equality except for the lightest case $m \simeq 10^{-26}$eV.

III. SFDM LINEAR PERTURBATIONS

The linear perturbations of scalar fields, and its influence in the CMB and other related observables, have been studied intensively in the specialized literature under a variety of different circumstances, see for instance[6, 7, 15, 20, 35, 36] and references therein. Here, we aim to

[1] It must be noticed that the equations of motion (8) are written with derivatives with respect to the number of e-foldings N. The derivatives can be changed to conformal time τ (the preferred time in CMB codes) via the well-known transformation $(d/d\tau) = aH(d/dN) = \mathcal{H}(d/dN)$, where $\mathcal{H}$ is the Hubble parameter itself given in terms of the conformal time

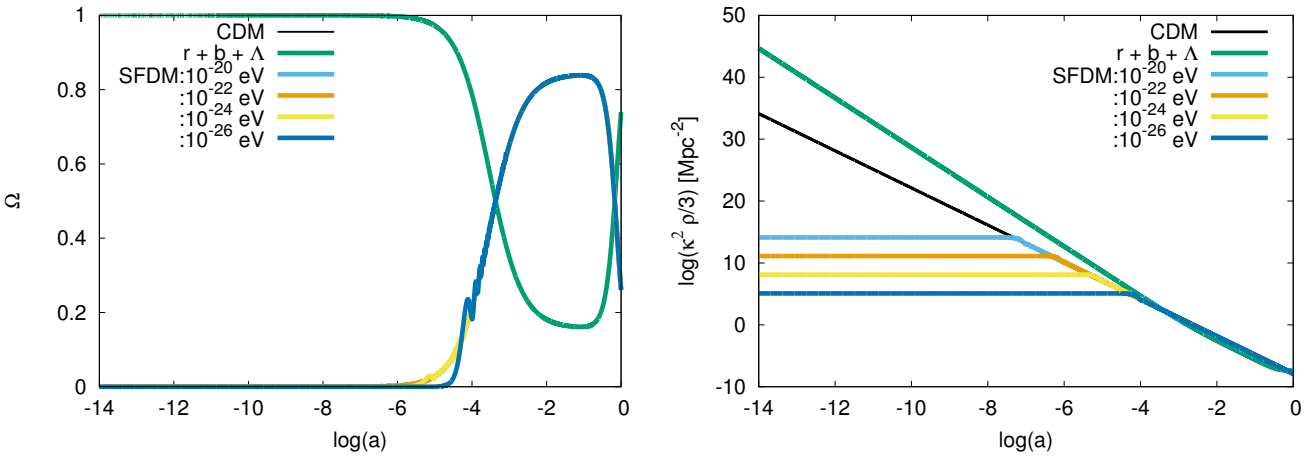

FIG. 1. Numerical solutions of the background equations (2) and (8) with a scalar field as dark matter at late times. The label CDM in the plots refers to the standard dark matter component, whereas r, b and Λ stand for radiation (photons and neutrinos), baryons, and a cosmological constant. Shown are: (Left) the density parameters Ω (see Eqs. (6)), and (Rigth) the energy densities ρ, of the different matter components. Notice that the standard evolution of the ΛCDM model is fully recovered at late times. The onset of the field oscillations is manifest in the wiggles present in the curves, although the most noticeable cases correspond to the lightest masses, for which the oscillations start very closely to the time of radiation-matter equality at $a \simeq 10^{-4}$. See Sec. II B for more details.

present a new study of field perturbations that, in many aspects, mirrors the one we presented for the background in Sec. II.

Following common wisdom, here we shall assume the synchronous gauge of metric perturbations, with the line element $ds^2 = -dt^2 + a^2(t)(\delta_{ij} + h_{ij})dx^i dx^j$. Notice that we will not work with the standard conformal time τ, and then a dot still means derivative with respect to the cosmic time t. The scalar field is given by $\phi(x,t) = \phi(t) + \varphi(x,t)$, where $\phi(t)$ is the background (homogeneous) field, and φ is its linear perturbation. Thus, the linearized KG equation for a Fourier mode $\varphi(k,t)$ reads[18, 35]:

$$\ddot{\varphi} = -3H\dot{\varphi} - (k^2/a^2 + m^2)\varphi - \frac{1}{2}\dot{\phi}\dot{h}\,, \qquad (20)$$

where h is the trace of scalar metric perturbations (with $\dot{h}$ known as the metric continuity), and k is a comoving wavenumber. The perturbations in density $\delta\rho_\phi$, pressure δp_ϕ, and velocity divergence θ_ϕ, are given, respectively, by[35, 37]:

$$\delta\rho_\phi = \dot{\phi}\dot{\varphi} + \partial_\phi V\,\varphi\,, \qquad (21a)$$

$$\delta p_\phi = \dot{\phi}\dot{\varphi} - \partial_\phi V\,\varphi\,, \qquad (21b)$$

$$(\rho_\phi + p_\phi)\theta_\phi = (k^2/a)\dot{\phi}\varphi\,. \qquad (21c)$$

The standard field approach for scalar field perturbations is to solve Eq. (20) for a given background evolution to find φ and $\dot{\varphi}$, which are then used to calculate the perturbative quantities (21). At a heuristic level, and for a rapidly oscillating scalar field, we can see that its linear perturbations grow if the fields in the KG equations (2c) and (20) have similar natural frequencies, which would happen for scales such that $k \ll m$, whereas in the opposite case $k \gg m$, we expect a suppression of the perturbations.

The true behavior of scalar field perturbations is actually more complex, and numerical solutions are unavoidable. However, Eq. (20) suffers from the same stiffness problem of the background equations, mainly because of the rapidly oscillatory terms that arise on the rhs from the presence of m^2 and $\dot{\phi}$, which also renders it impractical for numerical use in CMB codes[6, 7, 20]. An alternative, and second approach to the study of scalar field perturbations, is to transform Eq. (20) into an equivalent set of fluid equations, as was first done in the so-called formalism of generalized dark matter[37]. Such transformation is still impractical for numerical purposes (as already noted in[37]) in the case of rapidly oscillating scalar fields, mostly because some fluid terms, like the sound speed $c_s^2 = \delta p_\phi/\delta\rho_\phi$, are ill behaved during the oscillating phase of the scalar field.

Such difficulties in the fluid approximation have not deterred its ample use in the specialized literature[7, 12, 20, 35, 36]. One common corrective step in this method, that was firstly suggested in[18], is to assume an approximate ansatz for the field oscillations, and then to derive from it *averaged* fluid equations freed from any troublesome behavior[7, 20]. Although highly popular, this approach requires some intrusive pre-handling of the equations of motion that obscures the physical mechanisms at work in the evolution of SFDM perturbations.

We propose a third approach, based in a new field transformation of Eq. (20) quite similar to that we used

for the background variables:

$$u = \sqrt{\frac{2}{3}}\frac{\kappa\dot{\varphi}}{H} = -\Omega_\phi^{1/2} e^\alpha \cos(\vartheta/2)\,, \tag{22a}$$

$$v = \sqrt{\frac{2}{3}}\frac{\kappa m\varphi}{H} = -\Omega_\phi^{1/2} e^\alpha \sin(\vartheta/2)\,. \tag{22b}$$

For a simple interpretation of the new variables ϑ and α, it is useful to define the density $\delta_\phi \equiv \delta\rho_\phi/\rho_\phi$, and pressure $\delta_{p_\phi} \equiv \delta p_\phi/\rho_\phi$ contrasts, respectively, from the physical quantities (21). In summary, we find:

$$\delta_\phi = -e^\alpha \sin(\theta/2 - \vartheta/2)\,, \tag{23a}$$

$$\delta_{p_\phi} = -e^\alpha \sin(\theta/2 + \vartheta/2)\,, \tag{23b}$$

$$(\rho_\phi + p_\phi)\theta_\phi = -\frac{k^2}{am}\rho_\phi e^\alpha \sin(\theta/2)\sin(\vartheta/2)\,. \tag{23c}$$

The appearance of oscillations in the perturbative quantities can be easily spotted in Eqs. (23); they result from the combination of the background and perturbative angular variables θ and ϑ. Moreover, we can see that e^α can be simply interpreted as the amplitude of the scalar field density and pressure contrasts.

After long, but otherwise straightforward, calculations, we find that the equations of motion of the new variables, as derived from the perturbed KG equation (20), are:

$$\begin{aligned}\vartheta' = {} & 3\sin\vartheta + y_1 + 2\omega\sin^2(\vartheta/2) \\ & -2e^{-\alpha}h'\sin(\theta/2)\sin(\vartheta/2)\,,\end{aligned} \tag{24a}$$

$$\begin{aligned}\alpha' = {} & -\frac{3}{2}\left(\cos\vartheta + \cos\theta\right) - \frac{\omega}{2}\sin\vartheta \\ & +e^{-\alpha}h'\sin(\theta/2)\cos(\vartheta/2)\,.\end{aligned} \tag{24b}$$

There are two remarkable features in Eqs. (24). The first one is that the Hubble parameter H does not appear explicitly, and then the only connection of the perturbation variables to the background expansion is through the presence of θ and y_1. The second feature is that y_1, in a similar way as in Eq. (8a), should at some point become the dominant term in Eq. (24a), and then we must expect that at late times $\vartheta \simeq \theta$. Hence, the perturbation variables φ and $\dot{\varphi}$, see Eqs. (22), will also be rapidly oscillating functions just as their background counterparts.

Interestingly enough, Eqs. (24) quite naturally indicate the presence of a characteristic wavenumber in scalar field perturbations. For simplicity, we have denoted the ratio $\omega = k^2/k_J^2$, where

$$k_J \equiv a\sqrt{mH}\,, \tag{25a}$$

Notice that k_J is a time-dependent quantity that has been previously identified, sometimes just heuristically, as the comoving Jeans wavenumber of linear perturbations in scalar field models, see[6, 7, 20, 37, 38] and references therein. Its present, and then physical, value is:

$$\frac{k_{J0}}{\mathrm{Mpc}^{-1}} = 0.68\left(\frac{m}{10^{-23}\mathrm{eV}}\right)^{1/2}\left(\frac{H_0}{\mathrm{km\,s^{-1}\,Mpc^{-1}}}\right)^{1/2}. \tag{25b}$$

Actually, if the initial conditions are given in RD, we find that the variation of the Jeans wavenumber is just proportional to the present density parameter of radiation: $k_{Ji}/k_{J0} = a_i\sqrt{H_i/H_0} = \Omega_{r0}^{1/4}$. This also means that in a typical cosmological evolution $k^2/k_J^2 \lesssim 1$ for most of the scales of interest in structure formation, except in the case of extremely light masses $m \ll 10^{-23}$eV. A complete study of the effects of the Jeans wave number k_J in the evolution of SFDM perturbations will be presented in Sec. IV below.

A. Early time behavior

As for the background case, it is convenient to make a description of the early time behavior of the scalar field perturbations from the point of view that Eqs. (24) is a dynamical system, with at least one meaningful critical point as $a \to 0$ ($N \to -\infty$), which will then act as the source point for the physical solutions. In contrast to the background equations (8), the dynamical system (24) is not autonomous due to the presence of the background quantities θ and y_1, and the metric term h', which together act as an external time-dependent force term for the perturbations.

If we assume RD, then we know from Eqs. (10) that the behavior of the background variables in terms of the scale factor is: $5\theta = y_1 = y_i(a/a_i)^2$, whereas that of the metric perturbation must be $h = h_i(a/a_i)^2$, where h_i is a constant. This last expression comes from the well known solutions of linear perturbations in a RD universe with adiabatic initial conditions, see for instance[20, 35] for more details In order to find their critical point, we rewrite Eqs. (24) in the form:

$$\begin{aligned}\vartheta' = {} & 2\sin(\vartheta/2)\left[3\cos(\vartheta/2) + \omega\sin(\vartheta/2)\right. \\ & \left.-e^{-\alpha}h'\sin(\theta/2)\right] + y_1\,,\end{aligned} \tag{26a}$$

$$\begin{aligned}\alpha' = {} & \cos(\vartheta/2)\left[-3\cos(\vartheta/2) - \omega\sin(\vartheta/2)\right. \\ & \left.+e^{-\alpha}h'\sin(\theta/2)\right] + 3\sin^2(\theta/2)\,.\end{aligned} \tag{26b}$$

By simple inspection in Eq. (26a), we see that one critical point as $a \to 0$ is $\vartheta = 0$. If we substitute this value into Eq. (26b) we find that:

$$\alpha' \simeq -3 + e^{-\alpha}h'\sin(\theta/2) + 3\sin^2(\theta/2)\,. \tag{26c}$$

If we drop the last term in Eq. (26c) for being of a higher order in perturbations, we find that a first integral is: $e^\alpha \simeq (2/7)h\sin(\theta/2)$. Whereas ϑ reaches a true critical value, the critical condition on α just indicates its asymptotic behavior close to the point $a = 0$: $\alpha \sim 4N$ [2].

[2] In this respect, we cannot find a true critical point in the phase space spanned by the variables (ϑ, α). However, the critical point exists, at least formally, if the dynamical variables are (ϑ, e^α), and would correspond to $(\vartheta = 0, e^\alpha \to 0)$.

We can now calculate the solution of ϑ to the next order close to the critical point. Considering a perturbation of the form $\vartheta = 0 + \delta\vartheta$, then we find that at the lowest order Eq. (26a) becomes: $\delta\vartheta' = -4\delta\vartheta + y_1$, from which we readily obtain that the growing solutions is $\delta\vartheta = (1/6)y_1 = (5/6)\theta$. Therefore, the early-time solutions of the scalar field perturbations are represented by the expressions:

$$\vartheta = (5/6)\theta\,, \quad e^{\alpha} = (1/7)h\theta\,. \tag{27}$$

Eqs. (27) can be considered the *attractor* solutions of SFDM perturbations in the very early universe, and from them we can extract the right initial conditions for the scalar field perturbations. One important property of Eqs. (27) is that they do not depend on the wavenumber k, and then they are of general applicability for all scales.

Notice also that Eqs. (27) mean that the behavior of the scalar field density contrast close to the critical point, from Eq. (23a), can be cast in the form

$$\delta_\phi \simeq -\frac{1}{21}h\sin^2(\theta/2) = -\frac{1}{42}h(1+w_\phi)\,, \tag{28a}$$

and then the adiabatic condition $\delta_\phi = 0$ is accomplished as the scalar field EoS $w_\phi \to -1$ (see Eq. (7)) for $a \to 0$[20, 35]. Likewise, we can calculate the asymptotic expressions for the pressure contrast and the velocity divergence; from Eqs. (23b) and (23c) we find, respectively, that:

$$\delta_{p_\phi} \simeq -\frac{11}{21}h\sin^2(\theta/2) = -\frac{11}{42}h(1+w_\phi) \tag{28b}$$

$$(\rho_\phi + p_\phi)\theta_\phi \simeq -\frac{5}{21}\frac{k^2}{am}\rho_\phi h\sin^3(\theta/2)\,. \tag{28c}$$

We see that both quantities also vanish as $a \to 0$.

B. Gauge ambiguities and matter perturbations

One of the favourite gauges for the numerical evolution of perturbations is the synchronouns gauge, mostly for its reliability and straightforward formulation for different matter components. It is known, however, that this gauge can only be completely determined if additional constraints are taken into account. The standard procedure is to fix its remaining degree of freedom by considering that all calculations are performed in the comoving frame of the cold dark matter component, in which the corresponding velocity perturbation vanishes, i.e. $\theta_{CDM} = 0$[39]. It is clear that one must then be concerned about this gauge fixing in the cases where a scalar field is the dark matter, and specially if it is the only such component[40].

Most papers in the literature assume, under the fluid approximation of the equations of motion, that a rest framework can be established for SFDM much in the same way as for CDM; the physical condition that must be satisfied is

$$(\rho_\phi + p_\phi)\theta_\phi = 0\,. \tag{29}$$

This certainly can be done once the scalar field is oscillating and redshifting as matter[7, 20], but the concern about the gauge issue remains if one wishes to start a cosmological evolution well before the onset of the field oscillations. Although it is possible to consider the Newtonian gauge[15], or better a gauge-invariant evolution[21], we expect $(\rho_\phi + p_\phi)\theta_\phi \simeq 0$ for the whole evolution of the perturbations, and independently of the wavenumber k. As we shall see in Secs. IV C and IV D below, the velocity divergence of SFDM is zero for all practical purposes, which means that the synchronous calculations are actually made in the rest frame of the scalar field perturbations, and then the gauge ambiguity of SFDM is effectively canceled.

Finally, there is some concern also about the inclusion of SFDM perturbations into the matter spectrum, see for instance the discussion in Sec. IV B in[20]. Here we will adopt a conservative point of view, also implicitly assumed within the perturbations module of CLASS, that the term *matter perturbation* comprises the perturbations coming from all components behaving as CDM at late times. This criterion is certainly fulfilled by the SFDM models studied here, as they are all able to reach a cold matter behavior before the present time. Hence, in the definition of the matter spectrum we just write $\delta_m = (\delta\rho_b + \delta\rho_\phi)/(\rho_b + \rho_\phi)$ without making any distinction about the time before or after the onset of the field oscillations. One consequence of this is that the matter spectrum is mainly determined by the baryon perturbations at early times, but by the SFDM perturbations at late times once the scalar field dominates the matter sector.

C. Modifications in CLASS

The numerical evolution of the scalar field perturbations within CLASS is trickier than the evolution of the background, mainly because we need to take care of the different time scales that explicitly appear in the equations of motion, represented here by the angular variables θ, ϑ, and their combinations $\theta \pm \vartheta$. In order to make CLASS keep a good track of the evolution, it is convenient to use the following equations of motion that result from the combination of Eqs. (8a) and (24a):

$$\tilde{\vartheta}' \equiv (\theta-\vartheta)' = -3\left[\sin\theta+\sin(\theta-\tilde{\vartheta})\right] - \left[1-\cos(\theta-\tilde{\vartheta})\right]\omega + e^{-\alpha}h'\left[\cos(\tilde{\vartheta}/2)-\cos(\theta-\tilde{\vartheta}/2)\right] , \tag{30a}$$

$$\alpha' = -\frac{3}{2}\left[\cos(\theta-\tilde{\vartheta})+\cos\theta\right] - \frac{\omega}{2}\sin(\theta-\tilde{\vartheta}) + \frac{1}{2}e^{-\alpha}h'\left[\sin(\tilde{\vartheta}/2)+\sin(\theta-\tilde{\vartheta}/2)\right] , \tag{30b}$$

and then $\vartheta = \theta - \tilde{\vartheta}$. As anticipated in Sec. III, variables θ and ϑ will always have a very similar evolution, and then variable $\tilde{\vartheta}$, whose equation of motion (30a) does not contain y_1, will just measure the small difference between the two. Eqs. (30) together are the fundamental set of equations of motion for scalar field perturbations that were implemented in CLASS. The initial conditions for the new angular variables $(\tilde{\vartheta}, \alpha)$ are inferred from the attractor conditions (27), and then:

$$\tilde{\vartheta}_i = (1/6)\theta_i\,, \quad \alpha_i = \ln\left(h_i\theta_i/7\right) . \tag{31}$$

In order to deal with the rapidly oscillating terms in the perturbation equations, we also applied to them the cut-off procedure of Eq. (19), and then we made the replacements $\{\cos,\sin\} \to \{\cos_\star,\sin_\star\}$ for all the trigonometric functions in Eqs. (30) containing θ in the argument. Like in the case of the background variables, those trigonometric functions were numerically neglected once their corresponding arguments reached a high-frequency regime.

The equations of motion of perturbations were coded in CLASS following the formalism of the synchronous gauge, which is permitted as long as CDM is part of the matter budget. Our simulations considered that $\Omega_{CDM0} = 10^{-6}$, so that CLASS could still be able to fix the gauge completely. This is just a numerical trick because, as discussed in Sec. III B, the condition (29) for a rest framework of SFDM is always accomplished for all practical purposes.

In Figs. 2 we show the results from CLASS corresponding to the CMB temperature and mass power spectra, for the same range of masses as in the background dynamics: $10^{-26} < m/\mathrm{eV} < 10^{-20}$, and compare them with the standard ΛCDM model. In general terms, SFDM perturbations resemble very much those of the standard CDM plots, except for the lightest masses considered for which differences are more than noticeable. As for the matter spectrum, the most remarkable feature is the expected sharp cut-off for the smallest scales, which is clearly seen in the cases $m \lesssim 10^{-24}$eV, and that is in agreement with those already reported in the literature[6–8, 20].

IV. SUPPRESSION OF POWER IN SCALAR FIELD PERTURBATIONS

The common explanation for the suppression of power in the mass spectrum of SFDM is usually given in terms of the Jeans wave number (25), but still this is a confusing subject in the literature, mostly because of the different by-hand manipulations in the fluid approximation of the equations of motion. To illustrate the point, notice that we can write: $k^2/k_J^2 = (k^2/a^2m^2)(m/H)$, and then previous works have made separate and complicated studies of the perturbations in terms of the ratios k/am and m/H[7, 20, 21]. As we are to explain now, the linear equations (30) provide a simpler, though a bit subtler, explanation for the suppression of linear perturbations. The semi-analytic results below will be compared with the numerical ones obtained from the amended version of CLASS, which are shown in Figs. 3, 4 and 5 below.

A. General form of the equations of motion for scalar field perturbations

For a better visualization of the physics behind the evolution of scalar field perturbations, it is convenient to write the equations of motion (30) in the following form:

$$\begin{bmatrix} e^\alpha\cos(\tilde{\vartheta}/2) \\ e^\alpha\sin(\tilde{\vartheta}/2)\end{bmatrix}' = -\frac{3}{2}\begin{bmatrix} \cos\vartheta+\cos\theta+\frac{1}{3}\omega\sin\vartheta & -\sin\theta-\sin\vartheta-\frac{2}{3}\omega\sin^2(\vartheta/2) \\ \sin\theta+\sin\vartheta+\frac{2}{3}\omega\sin^2(\vartheta/2) & \cos\vartheta+\cos\theta+\frac{1}{3}\omega\sin\vartheta\end{bmatrix}\begin{bmatrix} e^\alpha\cos(\tilde{\vartheta}/2) \\ e^\alpha\sin(\tilde{\vartheta}/2)\end{bmatrix} + \frac{h'}{2}\begin{bmatrix}\sin\theta \\ 2\sin^2(\theta/2)\end{bmatrix} \tag{32}$$

To find the solutions of the field perturbations at early times, before the onset of the field oscillations, we just set $\vartheta = 0$ and retain the lowest order terms of θ in Eq. (32). The latter then becomes:

$$\begin{bmatrix} e^\alpha\cos(\tilde{\vartheta}/2) \\ e^\alpha\sin(\tilde{\vartheta}/2)\end{bmatrix}' \simeq -3\begin{bmatrix}1 & 0\\ 0 & 1\end{bmatrix}\begin{bmatrix} e^\alpha\cos(\tilde{\vartheta}/2) \\ e^\alpha\sin(\tilde{\vartheta}/2)\end{bmatrix} + \frac{h'}{2}\begin{bmatrix}\theta \\ \theta^2/2\end{bmatrix} . \tag{33}$$

If we again consider that during RD: $h = h_i(a/a_i)^2$ and $\theta = \theta_i(a/a_i)^2$, the growing solutions of Eq. (33) are:

$$\begin{bmatrix} e^\alpha\cos(\tilde{\vartheta}/2) \\ e^\alpha\sin(\tilde{\vartheta}/2)\end{bmatrix} \simeq \frac{h\theta}{7}\begin{bmatrix}1 \\ 7\theta/18\end{bmatrix} . \tag{34}$$

In agreement with the results in Sec. III A, inhomogeneities in the scalar field are then negligible at early times, mostly because θ diminishes the influence of the

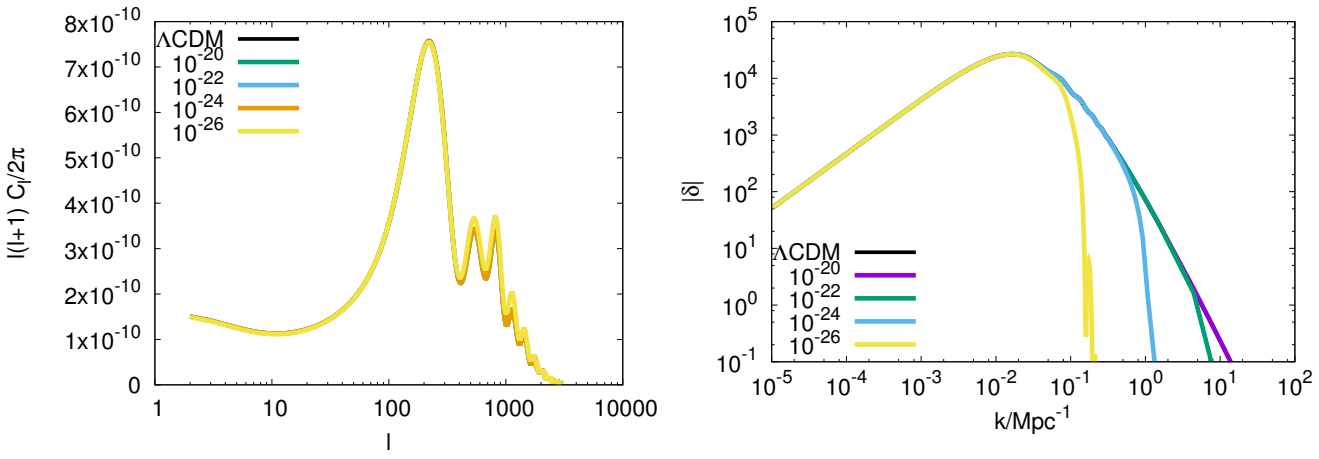

FIG. 2. (Left) CMB temperature and (Right) matter power spectra for ΛSFDM, as compared to the standard ΛCDM case. The differences are marginal for masses $m \gtrsim 10^{-24}$eV, but they become quite noticeable for the lightest cases. In particular, the most noticeable effect is the well-known cut-off seen in the mass power spectrum at large scales for the lightest massess considered in the examples. See the text for more details.

force term in Eq. (32). This situation can only be changed once the field approaches the onset of oscillations at $\theta = \pi/2$. Hence, we see that one reason for the suppression of power in the matter spectrum is the late appearance of the oscillations of the scalar field, and clearly such suppression is more acute for smaller values of the field mass m. This is a general effect that happens for all scales, as Eq. (33) is independent on the wavenumber k.

B. General solution of perturbations after the onset of the field oscillations

Once the field oscillations start, the dominant term on the right hand side of Eq. (24a) is y_1, which is a background variable that grows very rapidly, see Sec. II B. This readily indicates that at late times $\vartheta \simeq \theta$, and then any trigonometric function that depends on θ and ϑ must then be considered a *rapidly oscillating* function when compared with the expansion time H^{-1} of the Universe. In other words, we expect that:

$$\langle \sin\theta \rangle_{H^{-1}} = 0 = \langle \cos\theta \rangle_{H^{-1}} \,, \tag{35a}$$

$$\langle \sin\vartheta \rangle_{H^{-1}} = 0 = \langle \cos\vartheta \rangle_{H^{-1}} \,, \tag{35b}$$

where $\langle \cdots \rangle_{H^{-1}}$ means average over the Hubble time H^{-1}. Without such rapidly-oscillating trigonometric functions, Eq. (32) now becomes:

$$\begin{bmatrix} e^{\alpha}\cos(\tilde{\vartheta}) \\ e^{\alpha}\sin(\tilde{\vartheta}) \end{bmatrix}' \simeq \frac{\omega}{2}\begin{bmatrix} 0 & 1 \\ -1 & 0 \end{bmatrix}\begin{bmatrix} e^{\alpha}\cos(\tilde{\vartheta}/2) \\ e^{\alpha}\sin(\tilde{\vartheta}/2) \end{bmatrix} + \frac{h'}{2}\begin{bmatrix} 0 \\ 1 \end{bmatrix} . \tag{36a}$$

Eq. (36a) has the form of a forced harmonic oscillator with characteristic frequency $\omega/2$. In order to find approximate solutions, we will assume that $\omega = \text{const.}$, and then Eq. (36a) formally integrates into:

$$\begin{bmatrix} e^{\alpha}\cos(\tilde{\vartheta}/2) \\ e^{\alpha}\sin(\tilde{\vartheta}/2) \end{bmatrix} \simeq \begin{bmatrix} \cos(\omega N) & \sin(\omega N) \\ -\sin(\omega N) & \cos(\omega N) \end{bmatrix}\begin{bmatrix} C_1 \\ C_2 \end{bmatrix} + \frac{1}{2}\int_0^N d\hat{N} h' \begin{bmatrix} \sin[\omega(N-\hat{N})] \\ \cos[\omega(N-\hat{N})] \end{bmatrix} , \tag{36b}$$

where C_1, C_2 are integration constants, and $N = \ln(a/a_{osc})$. The integral on the rhs of Eq. (36b) can be made only if we know the form of the metric continuity h', which in turn can only be found after solving the full set of perturbation equations for all the matter fields.

As we are going to show now, a shortcut is to assume that we somehow know the behavior of the metric term h. In general, we will have two possibilities. The first one is to consider that $h = h_0 e^{\beta N}$, where $\beta > 0$ is a constant, and h_0 is the initial value of h. For instance, in the standard ΛCDM model we find that the growing solutions of the metric perturbations are of the form $h = h_0 e^{4N}$ ($h = h_0 e^{N}$) during RD (MD), and then we can assume that $h' = \beta h_0 e^{\beta N}$.

Likewise, in the case that matter perturbations are suppressed[3] we then expect that $h \simeq h_\infty + (h_0 - h_\infty)e^{\beta N}$, here h_0 (h_∞) are the values at $N \to 0$ ($N \to \infty$); in this case $\beta < 0$ and then $h' = \beta(h_0 - h_\infty)e^{\beta N}$. The general solution of Eq. (36b), in either of the aforementioned cases, can be written as:

$$\begin{bmatrix} e^\alpha \cos(\tilde{\vartheta}/2) \\ e^\alpha \sin(\tilde{\vartheta}/2) \end{bmatrix} \simeq \begin{bmatrix} \cos(\omega N) & \sin(\omega N) \\ -\sin(\omega N) & \cos(\omega N) \end{bmatrix} \begin{bmatrix} C_1 - \frac{\omega}{2(\beta^2+\omega^2)} h_0' \\ C_2 - \frac{\beta}{2(\beta^2+\omega^2)} h_0' \end{bmatrix} + \frac{h'}{2(\beta^2+\omega^2)} \begin{bmatrix} \omega \\ \beta \end{bmatrix} . \tag{36c}$$

The general solution then consists of an oscillating part plus an extra term proportional to the force term containing the metric perturbation. Before studying the general cases, we analyze the forced solutions without the oscillating terms. The separate solutions of the variables $\tilde{\vartheta}$ and e^α are, in full generality, given by:

$$\tan(\tilde{\vartheta}/2) \simeq \frac{\beta}{\omega} , \quad e^\alpha \simeq \frac{h'}{2(\beta^2+\omega^2)^{1/2}} . \tag{37a}$$

As we shall see now, there are only two *consistent* solutions if the scalar field perturbations are going to be the main source of matter perturbations.

The first one is what we call the *growing* case, which is achieved if $\omega \ll 1$ and e^α is a growing function. From the discussion above, this case corresponds to $h' = \beta h$, and then:

$$\tilde{\vartheta} \simeq \pi - 2\omega/\beta , \quad e^\alpha \simeq \frac{1}{2} h(1 - \omega^2/\beta^2) , \tag{37b}$$

where we have included the correction at the lowest order in $\omega/\beta \ll 1$. The first thing to notice is that the angular variable $\tilde{\vartheta} \to \pi$, and also $e^\alpha \to h/2$. In consequence, the scalar field density contrast at late times, from Eq. (23a), can be written as $\delta_\phi \simeq -(h/2)\cos(\omega/\beta) \simeq -h/2$. The solution is consistent in the sense that both the field perturbations and the metric continuity are growing functions. The numerical solutions corresponding to this case are shown in Fig. 3, for the wavenumbers $k = 10^{-4}, 10^{-1}\,\mathrm{Mpc}^{-1}$ and a scalar field mass $m = 10^{-24}\,\mathrm{eV}$.

The second possibility is the *decaying* case, for which $\omega \gg 1$ and e^α is a non-growing function. The latter condition can be achieved in the second case discussed above corresponding to $h' = \beta(h_0 - h_\infty)e^{\beta N}$, from which we obtain that:

$$\tilde{\vartheta} \simeq 2\beta/\omega , \quad e^\alpha \simeq \frac{1}{2(1+\omega^2/\beta^2)^{1/2}} (h_\infty - h) , \tag{37c}$$

where we included again the correction at the lowest order in $\beta/\omega \ll 1$. Eq. (37c) suggests that this time the angular variable $\tilde{\vartheta} \simeq 0$ for $|\beta/\omega| \ll 1$, and that the amplitude of perturbations vanishes, $e^\alpha \to 0$, as $h \to h_\infty$. The two results together imply that $\delta_\phi \to 0$. Like in the growing case, the new solution is also consistent in the sense that both the metric and field perturbations are non-growing functions.

However, as the force term in Eq. (36c) vanishes at late times for the decaying case, the true solution is eventually represented only by its oscillatory part. This is shown by the numerical solutions in Fig. 3 for the wavenumbers $k = 5, 10\,\mathrm{Mpc}^{-1}$, as it is for these values of k that $\omega \gg 1$ if $m = 10^{-24}\,\mathrm{eV}$.

Apart from the dynamical variables, there are two quantities that are of more physical interest: the scalar field density contrast δ_ϕ, and the velocity gradient θ_ϕ. In the following sections, we will analyze their behavior for large and small scales as compared to the Jeans wavenumber k_J.

C. Large scales $k \ll k_J$

For large enough scales $k \ll k_J$, the characteristic frequency of the oscillator (36a) is small at all times: $\omega \ll 1$. According to our discussion above, the only *consistent solution* for this case is the growing one represented by Eq. (37b), and then the complete solution for the scalar field density contrast, from Eqs. (23a) and (36c), is:

$$\delta_\phi = -e^\alpha \sin(\tilde{\vartheta}/2) \simeq -\left[C_1 - \frac{\beta^2}{2(\beta^2+\omega^2)} h_0\right] \sin(\omega N) - \left[C_2 - \frac{\beta\omega}{2(\beta^2+\omega^2)} h_0\right] \cos(\omega N) - \frac{\beta^2}{2(\beta^2+\omega^2)} h . \tag{38a}$$

[3] Such behavior of the metric perturbation h is expected if the perturbed Einstein equations are not sourced at all by any density

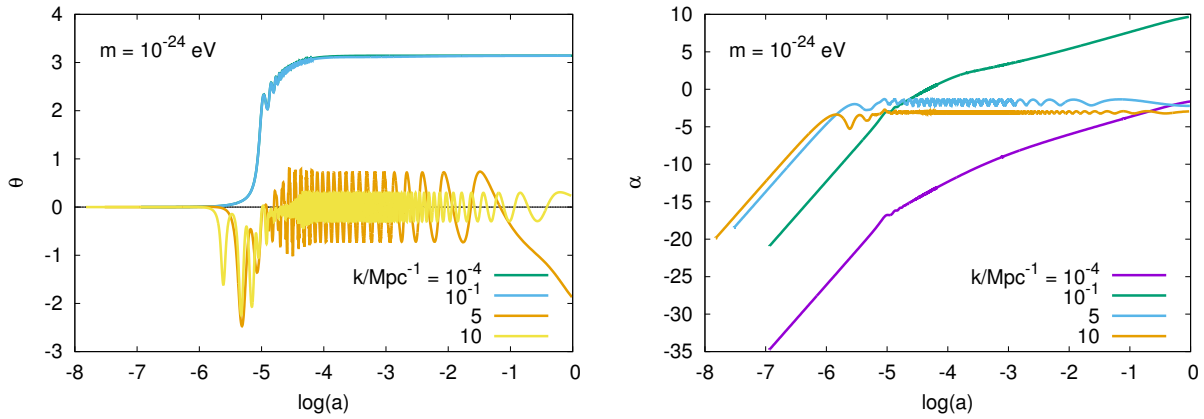

FIG. 3. Numerical solutions for the perturbation variables $\tilde{\vartheta}, \alpha$ for an example with a mass $m = 10^{-24}\,\mathrm{eV}$. For each variable we show two *growing* and two *decaying* cases, which correspond to the wavenumbers $k = 10^{-4}, 10^{-1}\,\mathrm{Mpc}^{-1}$, and $k = 5, 10\,\mathrm{Mpc}^{-1}$, respectively. The Jeans wavenumber for the given mass is, see Eq. (25b), and then the cases can also be distinguished by the value of the frequency ω: for the growing case $\omega \ll 1$, whereas $\omega \gg 1$ for the decaying one. In general, we can observe that for the growing case $\vartheta \to \pi$ and α grows, whereas for the decaying case both ϑ and α become oscillatory functions. The numerical solutions are in very good agreement with the semi-analytical results in Eqs. (36) and (37). See the text for more details.

If in addition $\omega \ll \beta$, this solution indicates that at late times, $\delta_\phi \simeq -h/2$, with some superimposed oscillations of small amplitude. Thus, SFDM behaves effectively as a pressureless component at the level of linear perturbations for large scales. This can also be corroborated from the calculation of the pressure contrast in Eq. (23b): $\delta_{p_\phi} = -e^\alpha \sin(\theta + \tilde{\vartheta}/2)$, from which we see that it is a rapidly oscillating function with a time-averaged value, calculated over a Hubble time, of $\langle \delta_{p_\phi} \rangle_H = 0$.

Finally, we can write the velocity gradient in Eq. (23c) in the form:

$$\theta_\phi \simeq \frac{k^2}{2am} e^\alpha \left[\cos(\tilde{\vartheta}/2) - \cos(\theta - \tilde{\vartheta}/2) \right] , \tag{38b}$$

where we also considered that $\langle p_\phi \rangle_H = 0$. Without the rapidly oscillating term, the velocity gradient is then represented by the first term in the solution (36c), and then:

$$\theta_\phi \simeq \frac{k^2}{2am} e^\alpha \cos(\tilde{\vartheta}/2) \simeq \frac{k^2}{2am} \left[\left(C_1 - \frac{\beta^2}{2(\beta^2+\omega^2)} h_0 \right) \cos(\omega N) + \left(C_2 - \frac{\beta\omega}{2(\beta^2+\omega^2)} h_0 \right) \sin(\omega N) + \frac{\beta\omega}{2(\beta^2+\omega^2)} h \right] . \tag{38c}$$

Apart from the superimposed oscillations of small amplitude, we see that the asymptotic solution at late times is:

$$\theta_\phi \simeq \frac{k^2}{4am} \frac{\omega}{\beta} h \simeq \frac{k^2 h_0}{4ma_{osc}} \frac{\omega}{\beta} , \tag{38d}$$

where the last term appears if $h = h_0 e^N$, which is expected during matter domination. Hence, the velocity gradient is also suppressed if $\omega \ll \beta$.

It must be recalled that the condition for large scales $k \ll k_J$ depends upon the value of the scalar field mass. In Figs. 4 and 5 we give numerical examples obtained from CLASS of the behavior of the density contrast δ_ϕ and of the velocity gradient θ_ϕ in comparison with those of other matter components. The large scale case correspond, in both figures, to the masses $m = 10^{-20}, 10^{-22}\,\mathrm{eV}$, and it can be clearly seen that both physical quantities evolve as suggested by the approximate solutions (38).

D. Small scales $k \gg k_J$

For the case of small enough scales, $k \gg k_J$, corresponding to $\omega \gg 1$, the consistent solutions at late times for the SFDM density contrast and velocity divergence, from Eq. (36c), are:

perturbations, see for instance Eqs. (21) in[39].

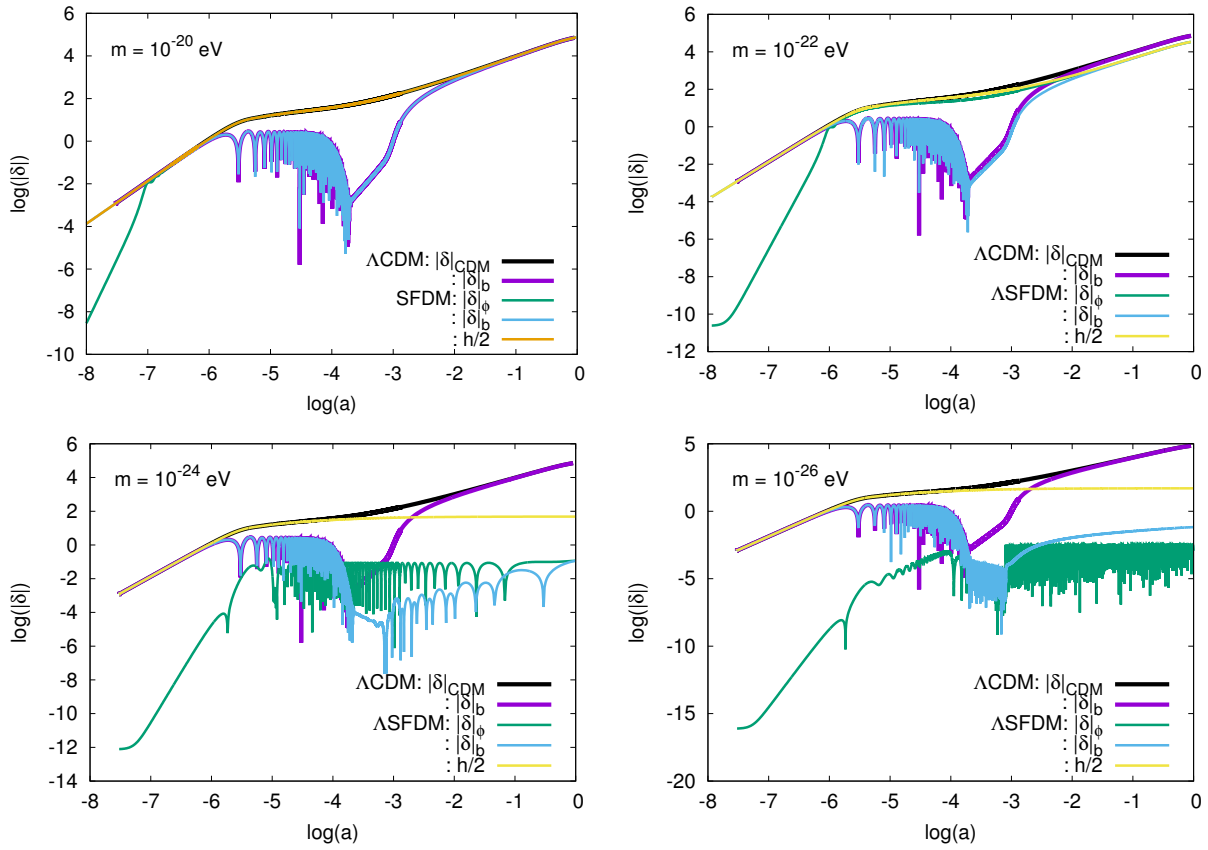

FIG. 4. The evolution of the density contrast of CDM, baryons (b), and SFDM (ϕ) for the same wavenumber $k = 5\text{Mpc}^{-1}$, as obtained from the amended version of CLASS for the different scalar field masses indicated in each one of the plots. As explained in the Secs. IV C and IV D below, the important parameter for the suppression of the scalar field perturbations is the ratio $\omega = k^2/k_J^2$, and then we refer to *large* (*small*) scales to the cases in which $\omega \ll 1$ ($\omega \gg 1$). Given that this ratio depends on the mass of the scalar field, one same scale can give $\omega \ll 1$ for large masses (e.g. $m = 10^{-20}, 10^{-22}$eV), or $\omega \gg 1$ for small masses (e.g. $m = 10^{-24}, 10^{-26}$eV). In general, SFDM perturbations evolve as those of CDM for the large scales, whereas they appear suppressed for the small scales. Also shown is the evolution of the metric perturbation $h/2$ (see Eq. (20)), which for late times accomplishes the relation $\delta_\phi = -h/2$ for large scales, whereas for small scales it approaches an asymptotic value: $h \to h_\infty$. See the text for more details.

$$\delta_\phi \simeq -\left[C_1 - \frac{\omega\beta(h_0 - h_\infty)}{2(\beta^2+\omega^2)}\right]\sin(\omega N) + \left[C_2 - \frac{\beta^2(h_0 - h_\infty)}{2(\beta^2+\omega^2)}\right]\cos(\omega N) + \frac{\beta^2(h_\infty - h)}{2(\beta^2+\omega^2)}\,, \tag{39a}$$

$$\theta_\phi \simeq \frac{k^2}{2am}\left[\left(C_1 - \frac{\omega\beta(h_0 - h_\infty)}{2(\beta^2+\omega^2)}\right)\cos(\omega N) + \left(C_2 - \frac{\beta^2(h_0 - h_\infty)}{2(\beta^2+\omega^2)}\right)\sin(\omega N) + \frac{\beta\omega(h_\infty - h)}{2(\beta^2+\omega^2)}\right]. \tag{39b}$$

In contrast to the case of large scales, this time the force term decreases as $h \to h_\infty$ and does not become the dominant part of the solutions. Instead, in the limit $\beta/\omega \ll 1$ we find that the true behavior of the physical quantities at late times is:

$$\delta_\phi \simeq -C_1\sin(\omega N) + C_2\cos(\omega N)\,, \tag{40a}$$

$$\theta_\phi \simeq \frac{k^2}{2am}\left[C_1\cos(\omega N) + C_2\sin(\omega N)\right]. \tag{40b}$$

Hence, the density contrast turns into a (highly) oscillating function of time with a small amplitude, with the latter inherited from the transition to the rapidly oscillating phase of the scalar field. The velocity gradient is also an oscillating function of time, but with a decreasing amplitude so that $\theta_\phi \sim a^{-1}$. Together with the results in the previous section, this reinforces our argument in Sec. III B that the velocity gradient of SFDM can be considered to be zero, for all practical purposes and for all scales, during the evolution of SFDM perturbations.

Numerical examples for small scales are also shown in Figs. 4 and 5 for the masses $m = 10^{-24}, 10^{-26}$ eV, and they agree very well with the approximate solutions in Eqs. (40): the density contrast is just an oscillating func-

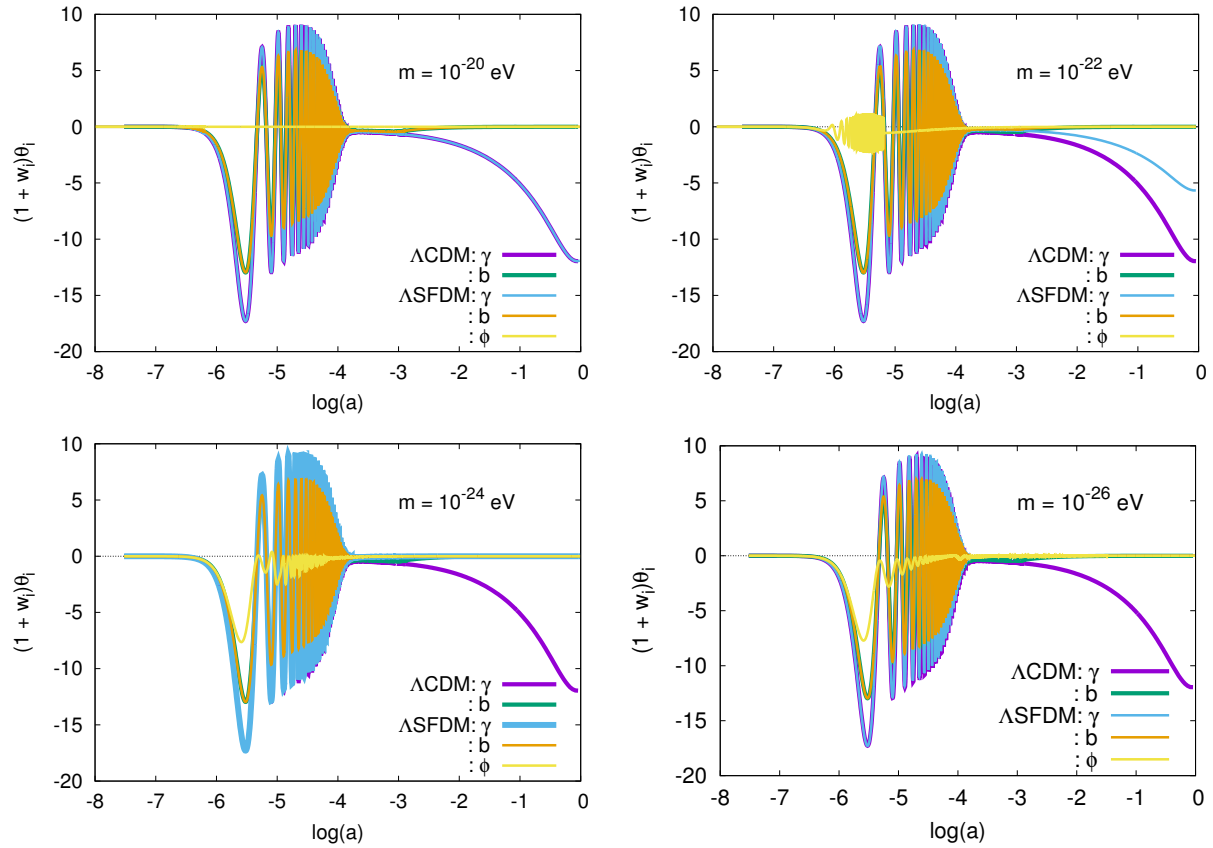

FIG. 5. The normalized velocity gradient $(1+w_I)\theta_I$ of different matter components for the same wavenumber $k = 5\,\mathrm{Mpc}^{-1}$ as in Fig. 4. That of a CDM component is not shown, as its velocity gradient is zero by definition in the synchronous gauge. The velocity gradient of photons and baryons, in the presence of SFDM, is the same as in ΛCDM for large scales, but not for small scales in which case all perturbations vanish. It is also confirmed that, for all practical purposes, the velocity gradient of SFDM is zero for both large ($\omega \ll 1$) and small ($\omega \gg 1$) scales. This justifies our analysis of SFDM perturbations in the synchronous gauge, as the calculations can be rightly considered as done in the rest framework of SFDM. As a side effect, notice that velocity gradient of the photons is also suppressed at late times, which is an expected result if $h' \to 0$ (see Eqs. (29) in[39]. For more details, see the text in Secs. III B, IV C, and IV D.

tion with a tiny amplitude, whereas the velocity gradient oscillates with a decaying amplitude.

V. POWER SPECTRUM AND MASS FUNCTION

In order to fully exploit the constraining power of future galaxy surveys such as DESI, LSST and Euclid for cosmological models, it is necessary to perform an accurate modeling of the matter power spectrum of any given dark matter models for wavenumbers up to $k \sim 10h\,\mathrm{Mpc}^{-1}$[41]. For ΛCDM models the standard perturbation theory provides good accuracy up to scales of $k \sim 0.1h\,\mathrm{Mpc}^{-1}$, while N-body simulations of structure formation are covering up to $k \sim 1h\,\mathrm{Mpc}^{-1}$.

In the case of the SFDM model studied here, up to now it was only possible to use approximate schemes to compute the mass power spectrum even at linear scales. With the novel method proposed in this work, we were able to describe the mass power spectrum at scales that can be considered in the semi-linear regime, without any by-hand approximations.

The standard approximation is to calculate the mass power spectrum for the SFDM model was to rescale the ΛCDM one using the expression:

$$P_{\mathrm{SFDM}}(k,z) = T^2(k,z) P_{\Lambda\mathrm{CDM}}(k,z) \tag{41}$$

where the transfer function T was effectively considered as redshift independent: [6, 7, 20, 37, 38],

$$T(k,z) = \frac{\cos(x^3)}{(1+x)^8} \quad x = 1.61 \left(\frac{m}{10^{-22}\mathrm{eV}}\right)^{1/18} \frac{k}{k_{J,eq}}\,, \tag{42}$$

where the Jeans scale $k_{J,eq}$ is the one given in Eq. (25b). In Fig. 6, we show the power spectrum calculated with the above expression (41), and the one calculated numerically in this work, and both of them are compared with the ΛCDM one. We can see that the relative difference

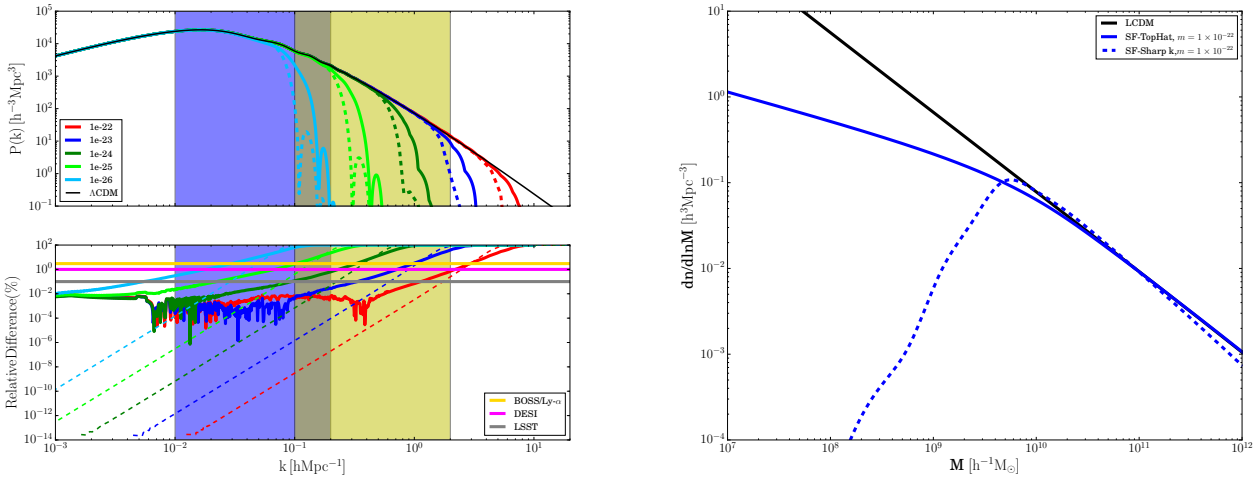

FIG. 6. (Left) Mass power spectrum for different masses of the scalar field as obtained from the amended version of CLASS (see also Fig. 2), in comparison with that of the ΛCDM model; also shown in comparison with the approximate expression (41) (dashed line). In the botton panel we plot the relative difference between the ΛCDM and ΛSFDM models, and show the constraining level from current and future galaxy surveys. The blue region are the scales proved by the galaxy power spectrum, and the yellow one by the Lyman-α power spectrum. (Right) Logarithmic derivative of the halo mass function for ΛCDM and $\Lambda SFDM$ (with $m = 10^{-22}$eV) using the Top-hat (continuous curve) and the Sharp-k (dashed curve) window functions. The suppression of structures below 10^{10} solar masses is more drastic if one uses a Sharp-k window function. See the text for more details.

between the last two is still small for large scales, laying below the 1% accuracy that will be achieved with DESI.

In particular scalar field models with masses smaller than 10^{-23} eV will not be discriminated by the shape of the mass power spectrum obtained from current galaxy and Lyma-α surveys. However, the region between $10^{-23} - 10^{-22}$eV could be proved by the next generation, specially if one includes the Lyma-α data. Also, as we can compute the power spectrum in the semi-linear scales with good accuracy, we can use the SFDM model to make predictions about other observables. This will be done detailed in future work, but for the present one we will show how the mass function is affected.

Previous studies of structure formation with small-scale suppression, particularly for Warm Dark Matter (WDM), have shown that the top-hat model fails in capturing the behavior of the cut-off in the power spectrum and how it translates into an almost complete suppression of the small scale structure. However, the Sharp-k window function seems to better reproduce the mass function from simulations. Some examples of these effects were shown in[42–44], and more recently in the simulations for the SFDM model done by [45] also showed the turn around in the mass function, that seems to be better described by a Sharp-k function than by the standard Top-hat. It must be noticed, though, that in[45] the initial conditions for the simulations were set up using the expression (41).

In Fig. 6, we show the halo mass function computed using the semi-analitical approach of Press-Schechter, with both the standard Top-hat window function and a Sharp-k function, for a scalar field mass of $m = 10^{-22}$eV; the ΛCDM result is also shown for comparison. We can note that the small mass scales are very sensitive to the choice of the window function, and further computations with will relay on it. Qualitatively, the sharp cut-off in the power spectrum translates into a small suppression in the mass function if a Top-hat function is used, while it translates in an also sharp cut-off in the mass function for the Sharp-k window. Since for the mass of our choice the sharp cut is occuring at mass scales smaller than 10^{10} Solar masses, we still expect it to be consistent with current numbers of observed satellite galaxies in the local group. A comprehensive analysis of how these differences propagate to the number of satellites in a Milky Way type galaxy is particularly interesting, but for now lies beyond the scope of this paper.

Finally it is worth to mention that both window functions need the input from numerical simulations of structure formation for a reliable computation of the halo mass function. The Sharp-k function needs it to set the mass scale at the turn-around, while the Top-hat needs it to set the q-value, which formally is a free parameter, in the first-crossing distribution. In that sense the two window functions need to be considering and at this point we can not tell which one is capturing the non-linear physics of the scalar field. For the examples in Fig. 6 we set the free paramteres in order to have a reasonable match of the mass function to the ΛCDM one at large mass scales, but it would be better to make use of structure formation

simulations.

VI. CONCLUSIONS

We have presented a new method to transform and solve numerically the equations of motion of a scalar field as a dark matter component. This method takes advantage of the explicit symmetries of the coupled Einstein-Klein-Gordon system of equations, and allow a clear understanding of the underlying physical solutions of the scalar field. The method is also suitable for numerical purposes, and deals correctly with the rapid oscillations of the field without any pre-handling of the equations of motion.

We showed that the background dynamics of SFDM is very simple in terms of the new dynamical variables, and even eases its numerical implementation in CMB codes, as exemplified with the results obtained from CLASS. Moreover, the transformation of variables used for the background case was easily adapted for the evolution of linear perturbations in the scalar field, and there was no need to rely on any similarities with standard fluid dynamics. The results for perturbations agree with previous results in the literature, but we were able to find semi-analytical solutions which show in a clear way the physical effects acting in the growing or suppression of linear perturbations.

The growing of perturbations in SFDM models for a given wave number k requires of two conditions: a) an early onset of field oscillations, preferably much earlier than the time of radiation-matter equality, and b) a negligible ratio k/k_J. Not surprisingly, both conditions depend upon the only free physical parameter which is the mass of the SFDM particle, and actually the two conditions are simultaneously enhanced (suppressed) in the case of large (small) values of m just because both angular variables θ and ϑ evolve similarly throughout.

As for condition b), we must recall first that the scales that have been affected at some degree by the Jeans wavenumber k_J, throughout the evolution of the Universe, are those for which initially $k/k_{J,eq} > 1$ with $k_{J,eq} = \Omega_{r0}^{1/4} k_{J0}$, see Eq. (25b). From this, we can infer that suppression of power, as compared to the standard CDM case, happens in scales:

$$\frac{k}{\mathrm{Mpc}} > 0.68\,\Omega_{r0}^{-1/4}\left(\frac{m}{10^{-23}\mathrm{eV}}\right)^{1/2}\left(\frac{H}{\mathrm{km\,s^{-1}\,Mpc^{-1}}}\right)^{1/2}. \tag{43}$$

This suggests, for instance, that for $m \geq 10^{-24}$eV even the slightest suppression of perturbations will lie at scales $k > 1\,\mathrm{Mpc}^{-1}$, an estimation that is in agreement with the numerical results shown in Fig. 2. In summary, for $m \geq 10^{-24}$eV the main source of suppression of SFDM linear perturbations is the Jeans length k_J, whereas for smaller values of m linear perturbations are also suppressed by the late appearance of the scalar field oscillations in the background.

We have recovered the results for SFDM perturbations that have been already reported in the literature under the fluid-approximation of the equations of motion for perturbations[7, 20]. However, we would like to emphasize that our method does not have a direct translation to the fluid-approximation, because some fluid quantities cannot be well defined in terms of our variables. An example we mentioned before is the sound speed of linear perturbations, which in our variables would be written as:

$$c_s^2 = \frac{\delta p_\phi}{\delta \rho_\phi} = \frac{\sin(\theta + \tilde{\vartheta}/2)}{\sin(\tilde{\vartheta}/2)}\,, \tag{44}$$

see also Eqs. (23). From our perspective, c_s^2 becomes a rapidly-oscillating function, which can also be ill-defined in the case of the small scales discussed in Sec. IV D. The connection of our variables to those of the fluid approximation is a topic that deserves further investigation, but we leave this issue for a future work.

Finally, we have explored some differences that appear in the mass power spectrum with respect to previous results published in the literature. The wavenumber at with which the cut-off of the power spectrum appears is consistent with reported results, but the suppression of power is not as sharp; this small differences can be significant for the determination of the mass function of small scale structure. The mass of the scalar field needs to be larger that 10^{-23}eV in order to be compatible with current power spectrum measurements, and future surveys will probably be able to prove the region $10^{-23}-10^{-22}$eV. Larger masses than 10^{-22}eV are incompatible with galactic dynamics. A further analysis of these constraints will be presented elsewhere.

ACKNOWLEDGMENTS

We want to thank Francisco Linares for a careful reading of the manuscript. LAU-L wishes to thank Andrew Liddle and the Royal Observatory, Edinburgh, for their kind hospitality in a fruitful sabbatical stay, where part of this work was done. AXG-M acknowledges support from Cátedras CONACYT and UCMEXUS-CONACYT collaborative proyect funding. This work was partially supported by PRODEP, DAIP, PIFI, CONACyT México under grants 232893 (sabbatical), 167335 and 179881, Fundación Marcos Moshinsky, and the Instituto Avanzado de Cosmología (IAC) collaboration.

Appendix A: Cut-off procedure for rapidly oscillating terms

In order to show the behavior of the numerical solutions under the cut-off procedure implemented for the trigonometric functions through Eq. (19), we present in Fig. 7 the cases of the scalar field energy density ρ_ϕ and

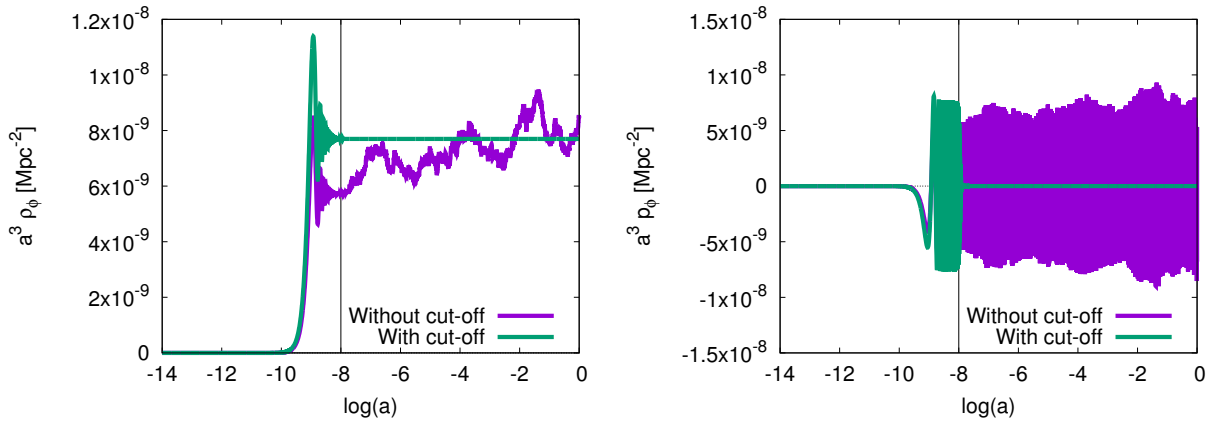

FIG. 7. (Left) The normalized energy density $a^3\kappa^2\rho_\phi/3$ in CLASS units, for a comparison between the cut and uncut cases of high frequency oscillations. We notice that the CLASS equation solver cannot give accurate numerical results for $a > 10^{-8}$, but the cut-off case gives a smooth transition to the correct solution at late times. (Right) The normalized pressure $a^3\kappa^2 p_\phi/3$ for the cut and uncut cases. The cut-off in the oscillations is more drastic in this case, although it can be seen that the pressure oscillates a bit erratically around zero in the full numerical solution, which signals the limitations of CLASS when dealing with stiff systems of equations. See the text and Sec. II D for more details.

pressure p_ϕ; the examples correspond to the same Universes shown in Fig. 1 with a mass of $m = 10^{-22}$eV. First of all, it can be seen that the uncut case cannot be handled appropriately by the equation solver within CLASS, and the evolution of the scalar field variables appears as erratic after the onset of the rapid oscillations. One undesirable consequence of this is that the present contribution of the scalar field, as given by $\Omega_{\phi 0}$, cannot be determined accurately enough from the given initial conditions discussed in Sec. II C.

The evolution with the cut-off implemented, on the other hand, is far more stable, and, in the case of the energy density ρ_ϕ, it matches smoothly the expected behavior at late times described in Sec. II B. In contrast to the uncut case, the present scalar field contribution $\Omega_{\phi 0}$ is given exactly as desired, and also determined uniquely in terms of the initial conditions (see Eq. (16). As for the scalar field pressure p_ϕ, it is drastically affected by the sudden cut-off of the oscillations in the scalar field EoS w_ϕ, but this does not have any major consequences for the overall evolution of all other cosmological variables. This again confirms that the cut-off procedure is a least invasive modification of the numerical computations as compared to the method of averaged quantities in the fluid approximation.

[1] P. Ade *et al.* (Planck Collaboration), (2015), arXiv:1502.02114 [astro-ph.CO].

[2] M. Vogelsberger, S. Genel, V. Springel, P. Torrey, D. Sijacki, D. Xu, G. F. Snyder, D. Nelson, and L. Hernquist, Mon. Not. Roy. Astron. Soc. **444**, 1518 (2014), arXiv:1405.2921 [astro-ph.CO]; S. Genel, M. Vogelsberger, V. Springel, D. Sijacki, D. Nelson, G. Snyder, V. Rodriguez-Gomez, P. Torrey, and L. Hernquist, Mon. Not. Roy. Astron. Soc. **445**, 175 (2014), arXiv:1405.3749 [astro-ph.CO].

[3] Y. Yang, Phys.Rev. **D91**, 083517 (2015), arXiv:1504.01195 [astro-ph.CO]; C. Angrick, F. Pace, M. Bartelmann, and M. Roncarelli, (2015), arXiv:1504.03187 [astro-ph.CO]; J. Barranco, A. Bernal, and D. Nunez, Mon.Not.Roy.Astron.Soc. **449**, 403 (2015), arXiv:1301.6785 [astro-ph.CO]; A. Cuoco, J.-Q. Xia, M. Regis, E. Branchini, N. Fornengo, *et al.*, (2015), arXiv:1506.01030 [astro-ph.HE].

[4] C. Amole *et al.* (PICO), Submitted to: Phys. Rev. D (2015), arXiv:1510.07754 [hep-ex]; V. Gluscevic, M. I. Gresham, S. D. McDermott, A. H. G. Peter, and K. M. Zurek, (2015), arXiv:1506.04454 [hep-ph]; A. Ringwald, (2015), arXiv:1506.04259 [hep-ph].

[5] S.-J. Sin, Phys.Rev. **D50**, 3650 (1994), arXiv:hep-ph/9205208 [hep-ph]; S. Ji and S. Sin, Phys.Rev. **D50**, 3655 (1994), arXiv:hep-ph/9409267 [hep-ph].

[6] T. Matos and L. A. Urena-Lopez, Class.Quant.Grav. **17**, L75 (2000), arXiv:astro-ph/0004332 [astro-ph]; Phys.Rev. **D63**, 063506 (2001), arXiv:astro-ph/0006024 [astro-ph]; T. Matos, A. Vazquez-Gonzalez, and J. Magana, Mon.Not.Roy.Astron.Soc. **393**, 1359 (2009), arXiv:0806.0683 [astro-ph].

[7] V. Sahni and L.-M. Wang, Phys.Rev. **D62**, 103517 (2000), arXiv:astro-ph/9910097 [astro-ph]; D. J. Marsh and P. G. Ferreira, Phys.Rev. **D82**, 103528 (2010), arXiv:1009.3501 [hep-ph]; D. J. E. Marsh and J. Silk, Mon.Not.Roy.Astron.Soc. **437**, 2652 (2013), arXiv:1307.1705 [astro-ph.CO]; T.-P. Woo and T. Chiueh, Astrophys.J. **697**, 850 (2009), arXiv:0806.0232 [astro-ph]; J.-c. Hwang and H. Noh, Phys.Lett. **B680**, 1 (2009), arXiv:0902.4738 [astro-ph.CO]; C.-G. Park, J.-c. Hwang, and H. Noh, Phys.Rev. **D86**, 083535 (2012),

arXiv:1207.3124 [astro-ph.CO].
[8] J. Beyer and C. Wetterich, (2014), arXiv:1407.0141 [astro-ph.CO].
[9] B. Li, T. Rindler-Daller, and P. R. Shapiro, Phys.Rev. **D89**, 083536 (2014), arXiv:1310.6061 [astro-ph.CO].
[10] L. A. Urena-Lopez, Phys.Rev. **D90**, 027306 (2014), arXiv:1310.8601 [astro-ph.CO].
[11] L. A. Urena-Lopez, JCAP **0901**, 014 (2009), arXiv:0806.3093 [gr-qc]; A. P. Lundgren, M. Bondarescu, R. Bondarescu, and J. Balakrishna, Astrophys.J. **715**, L35 (2010), arXiv:1001.0051 [astro-ph.CO]; A. Aguirre and A. Diez-Tejedor, (2015), arXiv:1502.07354 [astro-ph.CO].
[12] L. Amendola and R. Barbieri, Phys.Lett. **B642**, 192 (2006), arXiv:hep-ph/0509257 [hep-ph].
[13] T. Chiueh, (2014), arXiv:1409.0380 [astro-ph.CO]; J. Alexandre, (2015), arXiv:1502.03398 [hep-ph].
[14] E. J. Copeland, M. Sami, and S. Tsujikawa, Int.J.Mod.Phys. **D15**, 1753 (2006), arXiv:hep-th/0603057 [hep-th].
[15] D. J. E. Marsh, (2015), arXiv:1510.07633 [astro-ph.CO]; J. Magana, T. Matos, A. Suarez, and F. Sanchez-Salcedo, JCAP **1210**, 003 (2012), arXiv:1204.5255 [astro-ph.CO].
[16] T. Matos, J.-R. Luevano, I. Quiros, L. A. Urena-Lopez, and J. A. Vazquez, Phys.Rev. **D80**, 123521 (2009), arXiv:0906.0396 [astro-ph.CO].
[17] M. S. Turner, Phys.Rev. **D28**, 1243 (1983).
[18] B. Ratra, Phys.Rev. **D44**, 352 (1991).
[19] A. de la Macorra and G. Piccinelli, Phys.Rev. **D61**, 123503 (2000), arXiv:hep-ph/9909459 [hep-ph].
[20] R. Hlozek, D. Grin, D. J. E. Marsh, and P. G. Ferreira, (2014), arXiv:1410.2896 [astro-ph.CO].
[21] M. Alcubierre, A. de la Macorra, A. Diez-Tejedor, and J. M. Torres, (2015), arXiv:1501.06918 [gr-qc].
[22] L. Martinez-Medina, H. L. Bray, and T. Matos, (2015), arXiv:1505.07154 [astro-ph.GA]; L. Martinez-Medina, V. Robles, and T. Matos, Phys.Rev. **D91**, 023519 (2015), arXiv:1410.4163 [astro-ph.GA]; V. H. Robles, L. Martinez-Medina, and T. Matos, (2015), arXiv:1503.00799 [astro-ph.GA].
[23] V. H. Robles, V. Lora, T. Matos, and F. Sanchez-Salcedo, (2014), arXiv:1404.3424 [astro-ph.GA]; V. Robles and T. Matos, Phys.Rev. **D88**, 083008 (2013), arXiv:1302.5944 [astro-ph.CO].
[24] A. X. Gonzalez-Morales, A. Diez-Tejedor, L. A. Urena-Lopez, and O. Valenzuela, Phys.Rev. **D87**, 021301 (2013), arXiv:1211.6431 [astro-ph.CO]; A. Diez-Tejedor, A. X. Gonzalez-Morales, and S. Profumo, Phys.Rev. **D90**, 043517 (2014), arXiv:1404.1054 [astro-ph.GA].
[25] T. Rindler-Daller and P. R. Shapiro, Mon.Not.Roy.Astron.Soc. **422**, 135 (2012), arXiv:1106.1256 [astro-ph.CO]; Mod.Phys.Lett. **A29**, 1430002 (2014), arXiv:1312.1734 [astro-ph.CO].
[26] H.-Y. Schive, T. Chiueh, and T. Broadhurst, (2014), 10.1038/nphys2996, arXiv:1406.6586 [astro-ph.GA].
[27] K. Enqvist, S. Nadathur, T. Sekiguchi, and T. Takahashi, (2015), arXiv:1505.05511 [astro-ph.CO]; C. Boehm, A. Riazuelo, S. H. Hansen, and R. Schaeffer, Phys.Rev. **D66**, 083505 (2002), arXiv:astro-ph/0112522 [astro-ph].
[28] A. Mead and J. Peacock, Mon.Not.Roy.Astron.Soc. **440**, 1233 (2014), arXiv:1308.5183 [astro-ph.CO]; A. Mead, J. Peacock, L. Lombriser, and B. Li, (2014), arXiv:1412.5195 [astro-ph.CO]; L. Lombriser, F. Simpson, and A. Mead, (2015), arXiv:1501.04961 [astro-ph.CO].
[29] L. A. Urena-Lopez, (2006), arXiv:physics/0609181 [physics]; V. Faraoni and C. S. Protheroe, Gen.Rel.Grav. **45**, 103 (2013), arXiv:1209.3726 [gr-qc]; R. Garca-Salcedo, T. Gonzalez, F. A. Horta-Rangel, I. Quiros, and D. Sanchez-Guzmn, Eur.J.Phys. **36**, 025008 (2015), arXiv:1501.04851 [gr-qc].
[30] J. Lesgourgues, (2011), arXiv:1104.2932 [astro-ph.IM].
[31] E. J. Copeland, A. R. Liddle, and D. Wands, Phys.Rev. **D57**, 4686 (1998), arXiv:gr-qc/9711068 [gr-qc].
[32] M. J. Reyes-Ibarra and L. A. Urena-Lopez, AIP Conf.Proc. **1256**, 293 (2010).
[33] A. D. Rendall, Class.Quant.Grav. **24**, 667 (2007), arXiv:gr-qc/0611088 [gr-qc]; A. Alho and C. Uggla, (2014), arXiv:1406.0438 [gr-qc]; D. Blas, J. Lesgourgues, and T. Tram, JCAP **1107**, 034 (2011), arXiv:1104.2933 [astro-ph.CO]; J. Lesgourgues, (2011), arXiv:1104.2934 [astro-ph.CO].
[34] J. Martin, (2015), arXiv:1502.05733 [astro-ph.CO].
[35] P. G. Ferreira and M. Joyce, Phys.Rev.Lett. **79**, 4740 (1997), arXiv:astro-ph/9707286 [astro-ph]; Phys.Rev. **D58**, 023503 (1998), arXiv:astro-ph/9711102 [astro-ph]; F. Perrotta and C. Baccigalupi, Phys.Rev. **D59**, 123508 (1999), arXiv:astro-ph/9811156 [astro-ph]; H. Noh, C.-G. Park, and J.-c. Hwang, Phys.Lett. **B726**, 559 (2013), arXiv:1309.5692 [astro-ph.CO].
[36] D. J. E. Marsh, (2015), arXiv:1504.00308 [astro-ph.CO].
[37] W. Hu, Astrophys.J. **506**, 485 (1998), arXiv:astro-ph/9801234 [astro-ph].
[38] W. Hu, R. Barkana, and A. Gruzinov, Phys.Rev.Lett. **85**, 1158 (2000), arXiv:astro-ph/0003365 [astro-ph].
[39] C.-P. Ma and E. Bertschinger, Astrophys. J. **455**, 7 (1995), arXiv:astro-ph/9506072 [astro-ph].
[40] A. J. Christopherson, J. C. Hidalgo, and K. A. Malik, JCAP **1301**, 002 (2013), arXiv:1207.1870 [astro-ph.CO].
[41] A. Schneider, R. Teyssier, D. Potter, J. Stadel, J. Onions, D. S. Reed, R. E. Smith, V. Springel, and F. R. Pearce, (2015), arXiv:1503.05920 [astro-ph.CO].
[42] A. J. Benson, A. Farahi, S. Cole, L. A. Moustakas, A. Jenkins, M. Lovell, R. Kennedy, J. Helly, and C. Frenk, Mon.Not.Roy.Astron.Soc. **428**, 1774 (2013), arXiv:1209.3018.
[43] A. Schneider, Mon. Not. Roy. Astron. Soc. **451**, 3117 (2015), arXiv:1412.2133 [astro-ph.CO].
[44] M. R. Buckley, J. Zavala, F.-Y. Cyr-Racine, K. Sigurdson, and M. Vogelsberger, Phys. Rev. **D90**, 043524 (2014), arXiv:1405.2075 [astro-ph.CO].
[45] H.-Y. Schive, T. Chiueh, T. Broadhurst, and K.-W. Huang, (2015), arXiv:1508.04621 [astro-ph.GA].